High-Frequency Hubs of the Ictal Cross-Frequency Coupling Network Predict Surgical Outcome in Epilepsy Patients

Chunsheng Li, *Member, IEEE*, Abbas Sohrabpour, *Member, IEEE*, Haiteng Jiang, and Bin He, *Fellow, IEEE*

***Abstract*— Seizure generation is thought to be a process driven by epileptogenic networks; thus, network analysis tools can help determine the efficacy of epilepsy treatment. Studies have suggested that low-frequency (LF) to high-frequency (HF) cross-frequency coupling (CFC) is a useful biomarker for localizing epileptogenic tissues. However, it remains unclear whether the LF or HF coordinated CFC network hubs are more critical in determining the treatment outcome. We hypothesize that HF hubs are primarily responsible for seizure dynamics. Stereo-electroencephalography (SEEG) recordings of 36 seizures from 16 intractable epilepsy patients were analyzed. We propose a new approach to model the temporal-spatial-spectral dynamics of CFC networks. Graph measures are then used to characterize the HF and LF hubs. In the patient group with Engel Class (EC) I outcome, the strength of HF hubs was significantly higher inside the resected regions during the early and middle stages of seizure, while such a significant difference was not observed in the EC III group and only for the early stage in the EC II group. For the LF hubs, a significant difference was identified at the late stage and only in the EC I group. Our findings suggest that HF hubs increase at early and middle stages of the ictal interval while LF hubs increase activity at the late stages. In addition, HF hubs can predict treatment outcomes more precisely, compared to the LF hubs of the CFC network. The proposed method promises to identify more accurate targets for surgical interventions or neuromodulation therapies.**

***Index Terms*— Cross-frequency coupled network, epileptogenic network, high-frequency hub, stereo-electroencephalography (SEEG), surgical outcome.**

I. Introduction

EPILEPSY is one of the most prominent neurological diseases. Epileptogenic networks, which may be coordinated by different neuronal oscillations, represent the underlying seizure dynamics. Studying these networks with appropriate analysis tools helps delineate the epileptogenic tissues in the brain [1]–[3]. Identifying and characterizing the epileptogenic networks has a strong impact upon the surgical treatment of patients with intractable epilepsy [4]–[6]. High-frequency oscillations (HFOs, $>$ 30 Hz) have been proposed as a biomarker for defining epileptogenic tissues in focal epilepsy [7]–[10]. Epilepsy network in the gamma band was closely correlated with improved postsurgical outcome [11]. However, ictal HFO activities are widespread and are not limited to seizure foci and encompass the entire recorded network [12]. Moreover, HFOs are also present in intracranial EEG recordings covering normal brain tissues [13], [14], which suggests that HFOs alone cannot distinguish epileptic regions from nonepileptic regions sufficiently well. Low-frequency oscillations (LFOs, $<$ 30 Hz) were also reported to be highly correlated with epileptic activity [15]. For example, interictal regional delta (0.5–4 Hz) slowing has been suggested as a marker of epileptic networks in patients with temporal lobe epilepsy [16]. Additionally, global synchrony and local heterogeneity of interictal delta network were suggested as promising biomarkers for pediatric epilepsy surgery [17]. Although some progress is made in analyzing epileptogenic networks at individual frequencies, the understanding of interactions across different frequency bands is still limited and much needed.

A number of studies have suggested that resection of regions showing coupling between HFO amplitudes and LFO phases during seizure or sleep was linked to favorable outcomes in electrocorticographic (ECoG) recordings [18]–[23]. Ibrahim *et al.* reported that cross-frequency coupling (CFC) between pathological HFOs and the phase of theta and alpha rhythms was significantly elevated in the seizure-onset zone compared to non-epileptic regions [24]. Ictal early phase-locked high gamma (80–150 Hz) was suggested as an accurate indicator of post-operative outcome [23]. An eigen value decomposition method was also reported to analyze the ictal CFC in extratemporal lobe patients, and the results suggested that delta-modulated HFOs can be used to identify the epileptogenic zone [25]. Studies of noninvasive EEG also suggest that the CFC features observed in the scalp EEG can also predict seizure onset and localize the epileptogenic sources [26], [27]. Most studies, however, relied on

Manuscript received December 30, 2020; revised April 29, 2021 and June 16, 2021; accepted June 21, 2021. Date of publication June 30, 2021; date of current version July 12, 2021. This work was supported in part by the National Natural Science Foundation of China under Grant 61771323. *(Corresponding author: Chunsheng Li.)*

Chunsheng Li is with the Department of Biomedical Engineering, Carnegie Mellon University, Pittsburgh, PA 15213 USA, and also with the Department of Biomedical Engineering, Shenyang University of Technology, Shenyang, Liaoning 110817, China (e-mail: lichunsheng@sut.edu.cn).

Abbas Sohrabpour, Haiteng Jiang, and Bin He are with the Department of Biomedical Engineering, Carnegie Mellon University, Pittsburgh, PA 15213 USA.

This article has supplementary downloadable material available at https://doi.org/10.1109/TNSRE.2021.3093703, provided by the authors.

Digital Object Identifier 10.1109/TNSRE.2021.3093703

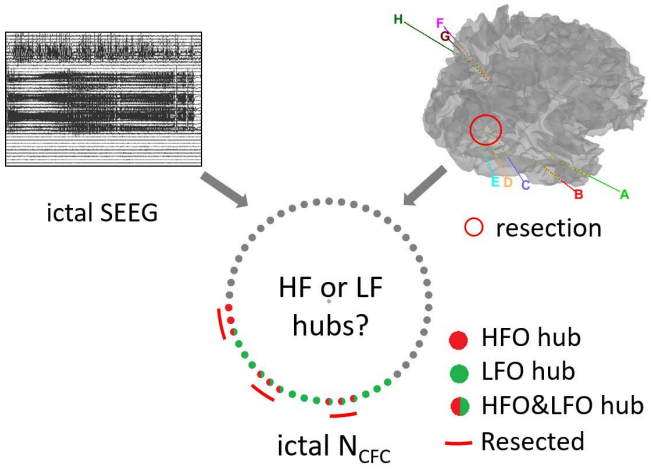

Fig. 1. We hypothesize that high-frequency (HF) hubs are more critical in determining treatment outcome compared to low-frequency (LF) hubs in ictal cross-frequency coupled networks (N_{CFC}).

the coupling strength of phase and amplitude between the time-course of activity at a specific region instead of the coupling network behavior, i.e. phase-amplitude coupling across different regions. Furthermore, it is still unclear whether the low-frequency (LF) hubs of CFC network are more critical for treatment outcome or the high-frequency (HF) hubs.

We investigated the dynamics of cross-frequency coupled network (N_{CFC}) during the ictal period, in which the amplitude of HFOs are coupled with the phase of LFOs across all possible pairs of electrodes. Furthermore, we hypothesize that the HF hubs of the N_{CFC} are primarily responsible for seizure generation compared to the LF hubs, which suggests HF hubs as a significant biomarker beneficial for planning respective surgery (Fig. 1). To test this hypothesis, we proposed a new approach for modeling the N_{CFC} and applied it to study the ictal spatiotemporal dynamics of Stereo-electroencephalography (SEEG) recordings in a cohort of epilepsy patients, to ultimately examine the relationship between N_{CFC} hubs and resected regions in focal epilepsy patients.

II. Materials and Methods

A. Data and Subject Description

Thirty-six seizures were recorded from SEEG electrodes in sixteen medically intractable epilepsy patients at Shenyang general hospital of military area. All seizures were classified as focal onset with impaired awareness seizures [28]. The inclusion criteria for subjects in this study were: 1. All patients underwent pre-surgical evaluation and had surgical or radio-frequency thermo-coagulation (RFTC) treatment; 2. All patients underwent SEEG recording during their pre-surgical evaluation; 3. Surgery outcomes are scaled by Engel Class (EC) with minimum 2 years' follow-up. Informed consent was obtained from each patient or their parents in the case of children or juveniles. This study was approved by the IRB of the Carnegie Mellon University (No. 2018_00000131). The clinical information of each patient is outlined in Table I.

SEEG recordings were performed using depth electrodes (0.8 mm diameter, 8–16 contacts per electrode each having a length of 2 mm, 1.5 mm intercontact distance). For electrode placement, a frameless stereotactic surgical robot, ROSA (MedTech, France), was used. Patients included in this study had more than two electrodes implanted on one hemisphere. Signals were sampled at 512 Hz or 1024 Hz with a 128-channel Nicolet EEG system (Natus Medical, USA). The recordings were referenced to a selected intracranial contact on white matter with minimum activity, which was placed as far as possible from suspected seizure generation and propagation regions. To eliminate the reference effect, SEEG recordings were transformed to a bipolar montage. Channels with obvious artifacts were removed based on visual inspection.

Patient specific CT images were used to verify the SEEG electrode positions. Resection/RFTC regions were marked by the neurologist. Surgical outcomes were ranked in EC (Table I). All surgical/RFTC treatments were based on clinical information before conducting this study. A neurologist examined the recordings and marked electrographic seizure onset and termination. We analyzed the ictal period to derive the N_{CFC}, and the results of graph measures and analyses were compared to the resected/RFTC regions of patients, for validation.

B. Phase Amplitude Coupling

The CFC in the form of phase-amplitude coupling (PAC) was computed [29], which assesses how much the phase of LFOs modulates the amplitude of HFOs. The time series of the amplitude envelope of higher frequency signals and the instantaneous phase of lower frequency signals were extracted from their respective continuous wavelet transform (CWT) spectra, which were obtained from the complex Morlet wavelet transform with a band width of 5 Hz and a center frequency of 0.8125 Hz [27]. The phase of lower frequencies (LF) was divided into N bins, and the amplitude of higher frequencies (HF) within each phase bin (k) was averaged (i.e.,$\langle A_{HF}^{LF}\rangle_k$). The mean amplitude was then normalized by dividing the sum of all mean amplitudes,

$$Q(j) = \frac{\langle A_{HF}^{LF}\rangle_j}{\sum_{j=1}^{N}\langle A_{HF}^{LF}\rangle_j}, \tag{1}$$

where N=18 for the number of phase bins, and the HFOs were chosen in the 30–150 Hz range in 5 Hz increments, whereas the LFOs were chosen in the 1–13 Hz frequency band in 0.5 Hz increments. The discrete probability density function of the normalized amplitude Q was then computed and compared with a uniform distribution by measuring the Kullback-Leibler (KL) distance. The KL distance was normalized to make all values fall between 0 and 1. If there was no PAC between low frequency and high frequency, then the amplitude distribution closed to a uniform distribution, which was reflected in a normalized KL distance of zero. A larger KL distance between Q and a uniform distribution was reflected in a larger PAC value. We used a 10 s sliding window with

TABLE I
CLINICAL INFORMATION OF PATIENTS STUDIED IN THIS WORK

P#	Age/Sex	Duration (years)	Seizure #	Seizure Duration (s)	MRI Findings	Pathology	Implantation Locations	Resection or RFTC	Surgical Outcome
P1	16M	10	3	66, 61, 48	Left hippocampal abnormality	FCD/ HS	Left: FTP	Left: T	EC I
P2	37M	17	3	74, 76, 77	Normal	FCD	Left: FTP	Left: T	EC I
P3	36M	23	1	75	Normal	Gliosis	Left: FT Right: T	Right: T	EC I
P4	31M	30	3	42, 64, 120	Multiple region abnormality	Gliosis	Left: T Right: FTP	Right: T	EC I
P5	25F	17	3	65, 97, 67	Normal	HS	Right: FTP	Right: T	EC I
P6	38M	32	1	71	Left occipital abnormality	–	Left: TPO	Left: O*	EC I
P7	11M	7	3	44, 54, 55	Left parietal and right occipital abnormality	Gliosis/FCD	Left: P Right: TO	Right: O	EC I
P8	54M	32	3	59, 60, 82	Right temporal abnormality	FCD	Right: FTP	Right: FT	EC I
P9	22M	3	1	76	both hippocampal abnormality	HS	Left: FT Right: FT	Left: T	EC I
P10	20F	6	3	20, 24, 22	Left parietal abnormality	Gliosis	Left: P Right: P	Left: P	EC I
P11	43M	30	1	80	Multiple ischemic lesions	Gliosis	Right: FTPO	Right: TP	EC II
P12	63M	25	2	128, 124	Left temporal and frontal atrophy	–	Left: FTPO Right: FTPO	Left: T* Right: T*	EC II
P13	3F	1	3	45, 55, 46	Left frontal abnormality, suspect FCD	–	Left: F	Left: F*	EC II
P14	37M	21	3	103, 118, 116	Normal	Gliosis	Left: FTPO	Left: P	EC II
P15	45M	16	2	30, 31	Normal	FCD	Right: FTP	Right: F	EC III
P16	41M	41	1	98	Left Hippocampal abnormality, parietal encephalomalacia	Gliosis	Left: FTPO Right: TP	Left: TP	EC III

F = frontal, T = temporal, P = parietal, O = occipital; * = radio-frequency thermo-coagulation (RFTC); – = unknown; P# = patient number; FCD = focal cortical dysplasia, HS = hippocampal sclerosis; EC = Engel Class.

step size of 1 s. A 10 s window was found to be the minimum window size required for reliably computing PAC [25], [30].

To determine statistical significance of PAC values, the surrogate method was employed [31]. A surrogate signal was created by randomly shuffling the amplitude of the original signal while keeping its phase the same. This process was repeated $N = 200$ times. The original PAC-gram was compared to its surrogate counterparts. If a pixel, i.e. frequency-frequency tile, in the PAC-gram was above the 95th percentile of the surrogate cases, the PAC value at this pixel was kept, otherwise, the original PAC pixel was set to zero. The surrogate procedure was performed when analyzing the whole seizure interval (not for the sliding window analysis).

C. Cross-Frequency Coupled Network (N_{CFC})

Cross-channel cross-frequency coupling with K channels of data will generate a four-dimensional matrix $X_{K\times(K-1)\times L\times H}$. Note that only the cross-channel PAC values were kept in this matrix and PAC values within channels were discarded, i.e. PAC of a channel with itself, since investigating coupling between cortical layers or regions may reduce the concerns on spurious PAC [32]. Subscript L and H represent the number of lower and higher frequencies chosen in the specified low and high frequency ranges, respectively. We reshaped the four-dimensional matrix by combining the first two indexes and the last two indexes independently. The reshaped two-dimensional matrix is represented in channel-pair vs. frequency-pair. By treating channel domain and frequency domain as independent dimensions, the principal component analysis (PCA) method was applied to the channel domain. We recovered the first PCA principal component as the principal PAC and the corresponding PCA contribution coefficients as the weighted N_{CFC}. Mathematically, the PCA can be expressed

as follows:

$$Y = PX = \begin{bmatrix} p_1 \cdot x_1 & \cdots & p_1 \cdot x_n \\ \vdots & \ddots & \vdots \\ p_m \cdot x_1 & \cdots & p_m \cdot x_n \end{bmatrix}, \quad (2)$$

where X is the reshaped two-dimensional zero-scaled PAC matrix, and P is the unmixing matrix; x_i represents the i^{th} frequency vector in X and p_j represents the j^{th} unmixing vector in P. y_1 is the first vector in column vector Y, which represents the first principal component. $m = K \times (K-1)$, and $n = L \times H$. p_1 is the coefficient to extract first principal component y_1 from X. Each element in p_1 corresponding to the contribution of each original channel to y_1. The absolute value of the p_1 was then re-shaped back to a $K \times K$ matrix, which forms the weighted N_{CFC}. The values of p_1 are determined by the PCA applied on PAC-grams, which are not limited the range of 0 and 1. The diagonal entries of the N_{CFC} was replaced with zeroes since we only use cross-channel PAC values. The strongest 5% of the total possible connections (corresponding to approximately 200 connections in a 64-channel montage) were set to 1 while the rest were set to 0, to construct the binary N_{CFC}, on which further analysis was performed [11].

D. Graph Analysis

Graph measures of in-degree and out-degree were calculated from the N_{CFC} to characterize the network. In-degree value indicates how much the HF activities of one node were phase modulated by other nodes in the N_{CFC}. We denote this measure as the HF hub. Out-degree value indicates the extent to which LF phase of one node were modulating HF amplitude of other nodes in the N_{CFC}, which we denote as the LF hub. The in-degree and out-degree of each node were normalized by the channel number of each network, and the average strength of hubs is 0.05. The strength of hubs lower than the average value was treated as less active hubs, and only values greater than the threshold were kept for further analysis. In-degree of the network was defined as:

$$D_{in}(j) = \frac{1}{K} \sum_{m=1, m \neq j}^{K} N_{mj} \quad (j = 1, 2, 3, \cdots, K), \quad (3)$$

and out-degree was defined as:

$$D_{out}(i) = \frac{1}{K} \sum_{m=1, m \neq i}^{K} N_{im} \quad (i = 1, 2, 3, \cdots, K), \quad (4)$$

where N_{ij} represents the principal coupling strength from LF node i to HF node j.

The Wilcoxon rank sum test was used to test the significant differences between the hub strength of resected and non-resected regions. All results were corrected by the Benjamini-Hochberg false discovery rate for multiple comparisons. The significance level was set at 0.01. All analyses were performed using MATLAB (MathWorks, Natick, USA). The first few seconds after ictal onset were excluded from hub analysis due to the absence of global coupling in the network at these early stages of the recording. The Brainstorm software package was used for data visualization [33].

III. Results

The processes of modeling N_{CFC} and applying graph measures are illustrated in Fig. 2. SEEG recording of one seizure from patient P1 is shown in Fig. 2(a). This temporal lobe epilepsy patients achieved seizure freedom after anterior temporal lobectomy. To capture ictal dynamics, the N_{CFC} of 10-second sliding windows shifted by 1 s were applied to each seizure recorded in this patient. A 10 s recording, marked by the blue rectangle in Fig. 2(a), was selected to calculate the cross-channel cross-frequency modulations, as shown in Fig. 2(b). The 4-dimensional matrices were then transformed to the principal PAC and the N_{CFC} by applying the PCA method detailed before, as shown in Fig. 2(c). The median frequency of LFO can be extracted from principal PAC, and it is 3.8 Hz in this patient as depicted in Fig. 2(c). The median frequency of LFO during the whole seizure can be extracted by sliding windows, as shown in Fig. S1, and it can be observed that the main seizure frequency changes dynamically, following seizure onset. The HF hubs and LF hubs of the N_{CFC} were plotted on patient's head model as shown in Fig. 2(d) and Fig. 2(e), and all strengths of HF hubs and LF hubs at each sliding window are plotted in Fig. 2(f) and Fig. 2(g), respectively. The HF hubs started emerging from the resected channels several seconds after seizure onset as demonstrated in Fig. 2(f). HF hubs also emerged outside of the resection volume, at the middle and late stages of the seizure, such as channel E3-1 located at the post cingulate cortex (PCC) of patient P1. Conversely, the LF hubs were more widely distributed outside of resection at the early stage, such as channel F3-1 and F7-5 located near the PCC.

A. Transition From the Pathological HF Hub to the LF Hub

The amplitudes of ictal HFOs are coupled with the phase of LFOs dynamically over time, frequency, and space. All seizures were divided into three stages (early, middle, and late) with equal number of sliding windows, basically dividing each seizure interval into 3 equal segments as shown in Fig. 2(f). Ictal dynamics can be seen from hubs shown on patient's head model, and also averaged during the three stages as depicted in Fig. S2. If patients had more than one seizure, the strengths of HF hubs and LF hubs were averaged over all analyzed seizures. The HF and LF hub values at each stage of the ictal period are grouped and displayed based on patient outcome in Fig. 3(a) and Fig. 3(b), respectively. In the EC I group ($n = 10$), the strength of HF hubs was significantly higher inside the resected regions compared to non-resected regions during early and middle stages of the seizure interval ($p < 0.001$). In the EC II group ($n = 4$), the strength of HF hubs was significantly stronger compared to non-resected regions at the early stage of the seizure interval ($p < 0.01$), while there was no significant difference in the EC III group ($n = 2$). Interestingly, the strength of LF hubs was significantly increased inside the resected regions at the late stage of ictal period in the EC I group ($p < 0.01$). Overall, these results indicate a transition from early dominance of

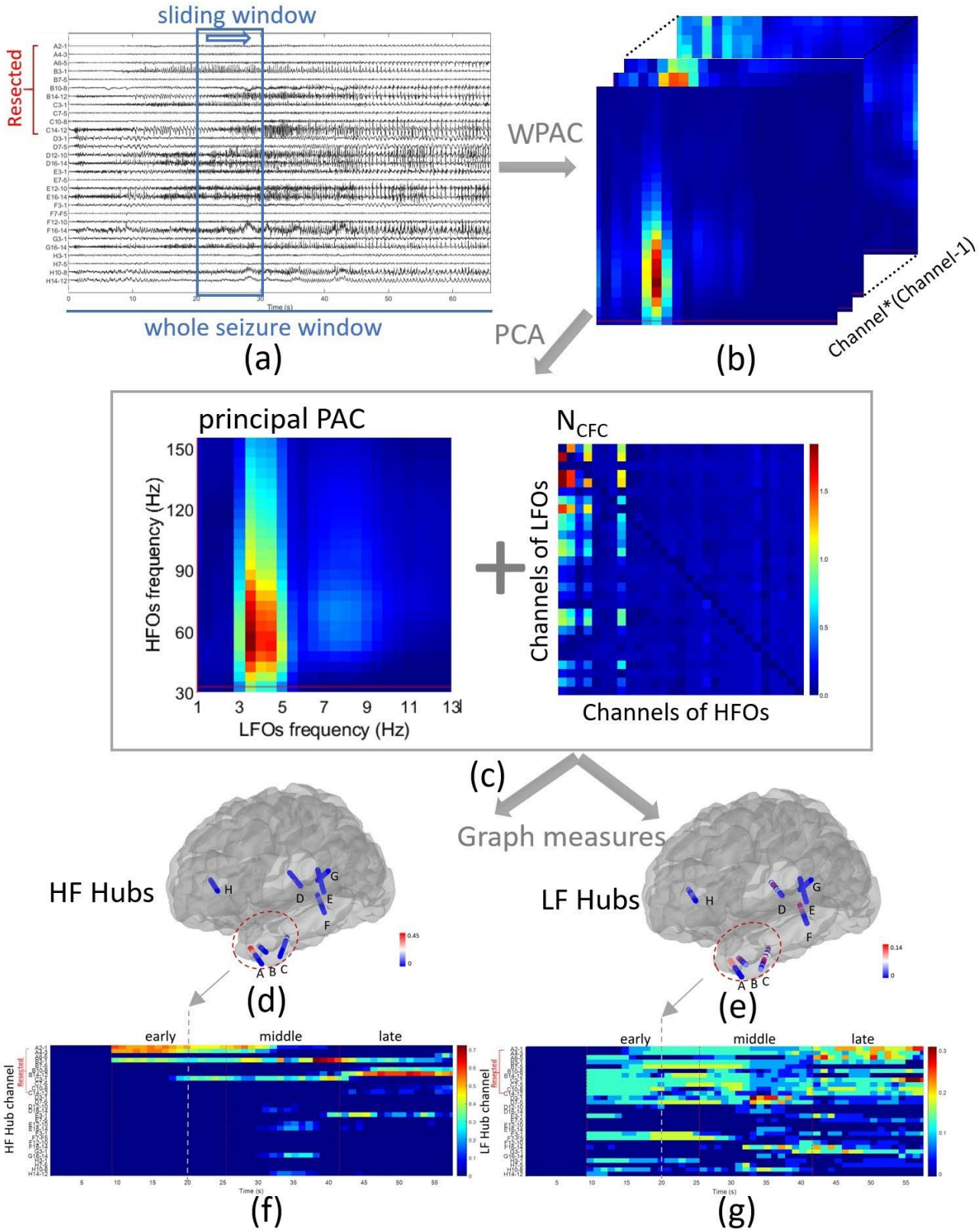

Fig. 2. An example of modeling cross-frequency coupled network (N_{CFC}) and applying graph measures. (a) SEEG recording of one seizure from patient P1. The blue rectangle indicates the segment used for generating (b)-(e). Resected channels are marked by the red bracket. (b) Cross-channel cross-frequency couplings obtained by wavelet phase-amplitude coupling (WPAC); lower frequency (phase) shown on the horizontal axis and higher frequency (amplitude) on the vertical axis. (c) The principal phase-amplitude coupling (PAC) and N_{CFC} extracted by PCA method from (b). (d) High-frequency (HF) hubs and (e) low-frequency (LF) hubs plotted on patient's head model, which are obtained by applying graph measures on the N_{CFC}. The SEEG contacts are enlarged for visualization. The resected region is marked by the red circle. (f) Strength of HF hubs and (g) LF hubs change with time and over different locations over different windows. (d) and (e) represent the HF and LF strengths for the time instance marked by the arrow in (f) and (g), respectively.

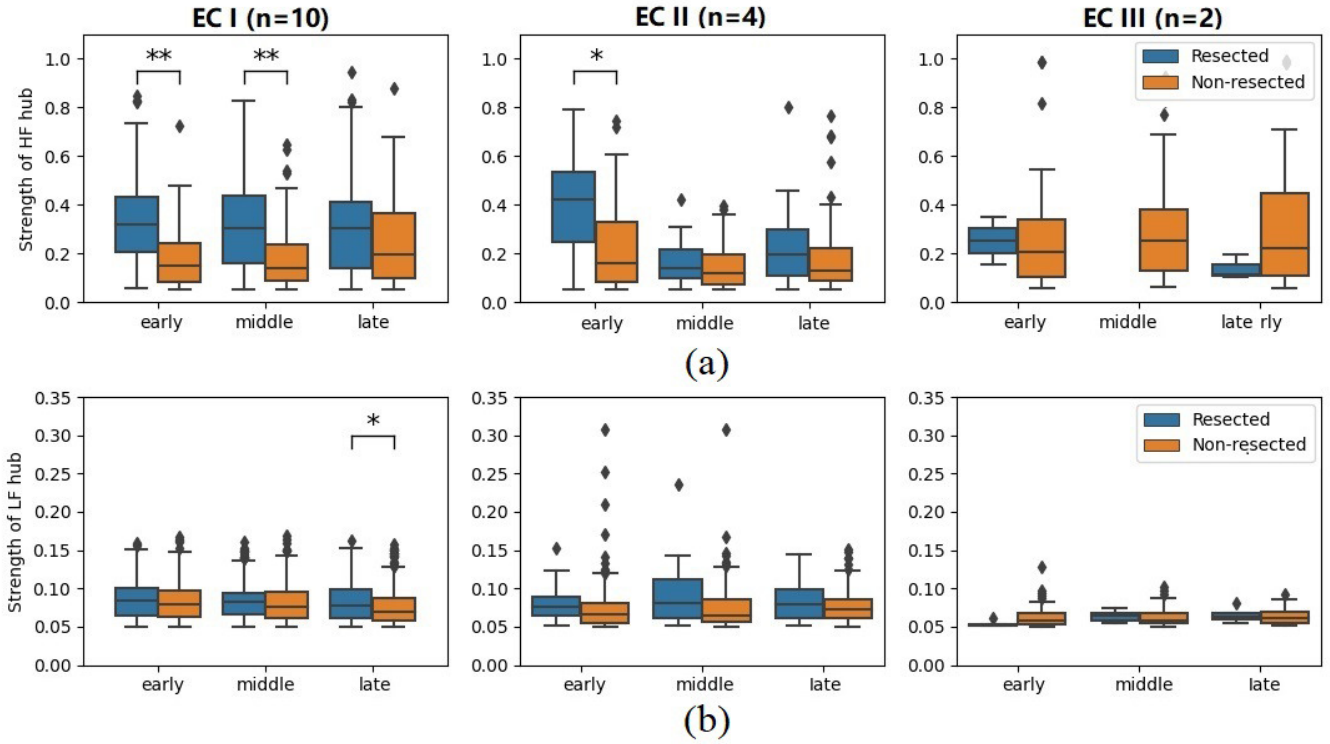

Fig. 3. The statistical results of the strength of high-frequency (HF) and low-frequency (LF) hubs changing in early, middle, and late stages. (a) Statistical analysis of the strength of the HF hubs in different ictal stages and in different outcome groups. The strength of HF hubs in resected regions is significantly higher than non-resected regions in early and middle stages of the EC I group ($*: p < 0.01$; $**: p < 0.001$). The same quantity is only significantly different for the early stage in the EC II group, and no such significance was found for the EC III group. (b) Statistical analysis of the strength of the LF hubs. The strength of LF hubs is only significantly higher than non-resected regions in the late ictal stage for the EC I group, while HF hubs show no such difference.

pathological HF hubs to later activities of the LF hubs in the ictal N_{CFC}.

B. Treatments on HF Hubs Correlate With Improved Outcomes

The N_{CFC} across the whole seizure was further analyzed. Note that no sliding window was used for the analyses presented in this section. The purpose of extending window size to the whole seizure interval including the first few seconds is to simplify the process. Surrogate analysis with cross-channel PAC values was employed in this part of the analysis, which decreases the chance of the extracted N_{CFC} being due to spurious activity [32], [34], [35]. SEEG electrodes were divided into four groups based on anatomical location, namely, into the temporal, frontal, parietal, and occipital groups. The HF hubs and LF hubs of all patients are plotted in Fig. S3(a) and S3(b). The strength of HF hubs inside resected regions were significantly higher than the hubs outside of the resected region in the EC I group ($p < 0.001$), as depicted in Fig. 4(a). There was no significant difference between HF hubs inside and outside of the resected region in the EC II and III groups. Moreover, significantly stronger LF hubs were found inside resected regions in the EC I group ($p < 0.01$), as shown in Fig. 4(c). To determine "active" or "inactive" hubs, a threshold of 3 dB below the maximum strength was chosen, i.e. 70% of peak amplitude. Notably, 92.5% of active HF hubs were resected, i.e. within the resection or ablated region, in the EC I group, compared to a mere 33.3% of active HF hubs resected in the EC II group (Fig 4(b)). Interestingly, no active HF hubs were resected in the EC III group. Therefore, the higher the percentage of the resected active HF hubs, the better the patient outcomes. In other words, the distribution of LF hubs was widely spread compared to the HF hubs, as illustrated in Fig S3(b). The percentage of active LF hubs within the resected regions was 56.4%, 4.5%, and 22.0% in the EC I, II, and III group, respectively (Fig. 4(d)).

Some studies suggest that HFOs alone cannot distinguish epileptic regions from nonepileptic regions [13], [14]. To further validate these results in our data, we performed directional spectral Granger analysis, using the directed transfer function (DTF) method [11], to analyze the roles of HFO and LFO networks, independently. The frequency ranges of HFO networks and LFO networks were extracted from principal PACs [27]. Only 58.8% of active HF hubs and 47.5% of active LF hubs determined from the DTF analyses resided in the resected regions of patients with EC I outcome (Fig. S4). Compare to the values obtained using the proposed approach, namely 92.5% of HF hubs and 56.4% of LF hubs, as reported in Fig. 4(b) and Fig. 4(d).

C. The Deep Region HF Hubs in Seizure-Free Group

There were six patients with temporal lobe epilepsy (TLE), who became seizure free after treatment. Depth of contact was measured from entry point of the SEEG electrode; so,

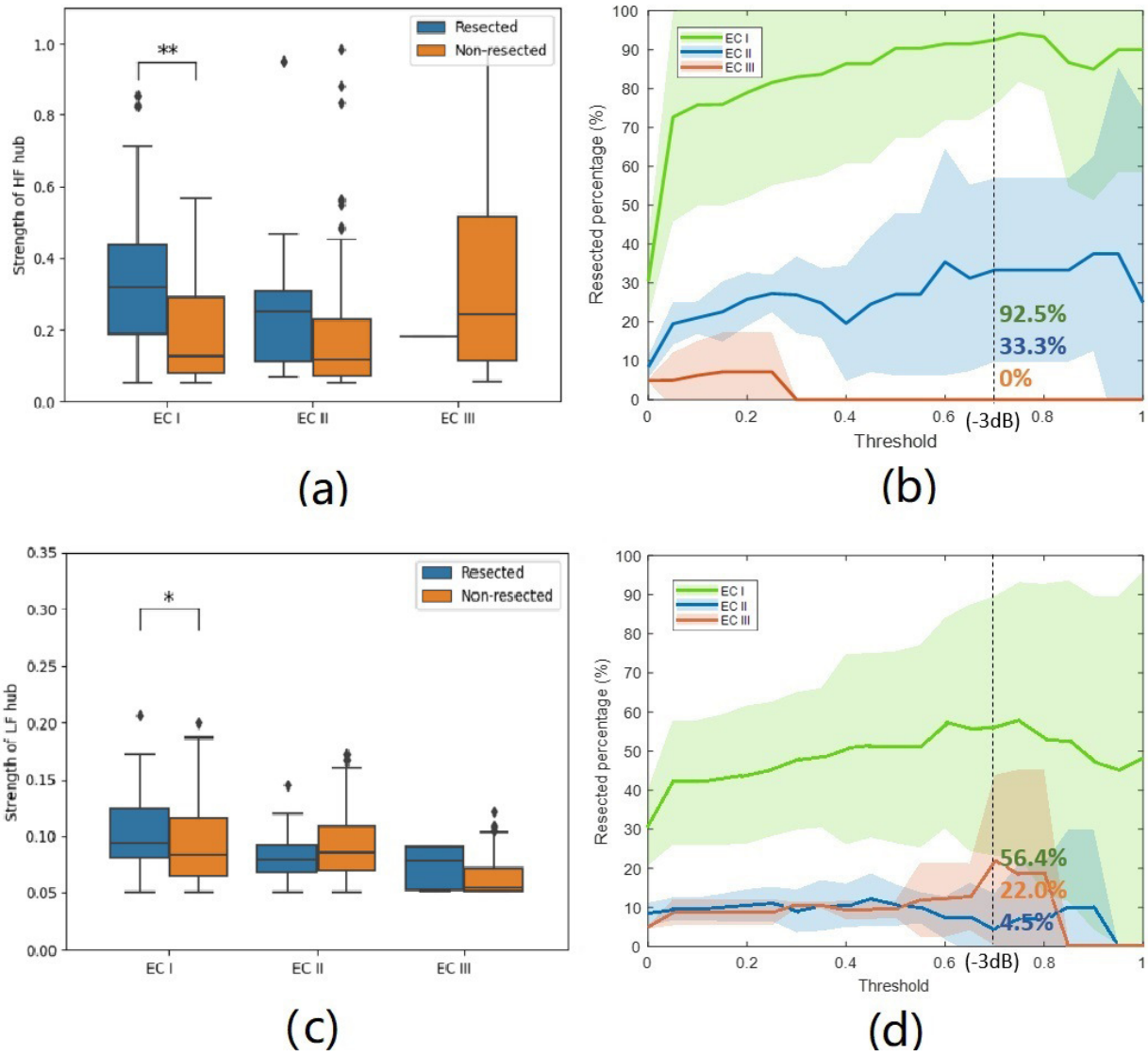

Fig. 4. High-frequency (HF) hubs and low-frequency (LF) hubs of the whole-seizure networks. (a) Statistical analysis of the strength of the HF hubs. There is a significant difference between resected hubs and non-resected hubs in the EC I group. (b) Percentage of HF hubs resected in different outcome groups. The threshold was set at 3 dB below maximum strength, 92.5%, 33.3%, and 0% of the HF hubs are resected in the EC I, II, and III groups, respectively. (c) Statistical analysis of the strength of the LF hubs. (d) Percentage of LF hubs resected in different outcome groups are 56.4%, 4.5%, and 22.0% for the EC I, II, and III groups, respectively.

the depth of the most superficial contact is zero. The HF hubs mostly resided in deep contacts. In these patients, 88.6% of the HF hubs were located in the contacts deeper than 10 mm (Fig. 5(a)). Based on the post-SEEG CT and pre-SEEG MRI images, we localized all SEEG electrodes and divided them into mesial structure, temporal pole region, and cortex in the sulcus based on their location. 34.1% of HF hubs were located at the mesial structure such as hippocampus, amygdala, and parahippocampal gyrus. The HF hubs at hippocampus were found in patients P1, P2, P4, and P5. The HF hubs at amygdala were found in patients P1, P5, and P9. 36.4% of HF hubs were located at the temporal pole region, which were found in all six TLE seizure-free patients, and 13.6% of HF hubs located at the sulcus of cortex. 95.8% of active HF hubs were located in the resected regions of the TLE patients, but this number is only 50% in patient P8 with both temporal and frontal lobes resection, as shown in Fig. 5(c). Further analysis on patient P8 showed that the other 50% of HF hubs are located 9 mm away from the boundary of resection (Fig. S5). In the three extra-temporal lobe epilepsy (ETLE) patients with seizure-free outcome, all identified HF hubs were located deeper than 10 mm (Fig. 5(b)). Patient P6 and P7 underwent RTFC and surgery on deep structures of occipital lobe respectively, and patient P10 underwent surgery on deep structure of parietal lobe, as shown in Table I. All active HF hubs were inside the treatment region (Fig. 5(c)).

IV. Discussion

A. N_{CFC} Properties

The N_{CFC} is an asymmetric network, in which each value represents the degree to which the LF phase from one channel is coupled with the HF amplitude from another channel. Binary network with 5% total connections were selected

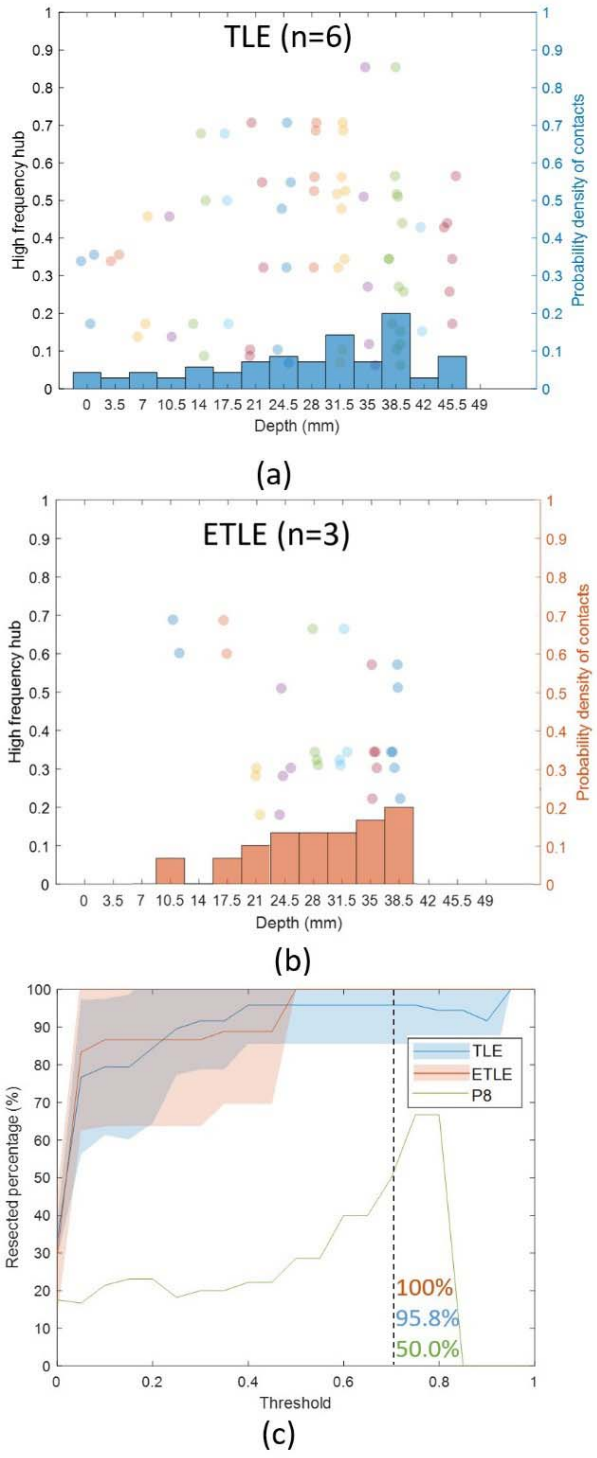

Fig. 5. High-frequency (HF) hubs in deep sources of the EC I group. (a) Distribution of HF hubs of temporal lobe epilepsy (TLE) patients in the EC I group. 88.6% of the hubs are distributed in depths larger than 10 mm. (b) Distribution of HF hubs in extra-temporal lobe epilepsy (ETLE) patients in the EC I group. All hubs were located deeper than 10 mm from cortical surface. (c) Percentage of the resected HF hubs that were above the threshold. All HF hubs above the threshold of 3 dB-below-max were resected in ETLE patients. 95.8% of HF hubs above the threshold were resected in TLE patients; in patient P8 with both temporal and frontal lobe resections, this number dropped to 50%.

here to guarantee the significance of the cross-channel coupling, and surrogate testing was also used to reject spurious couplings [32]. Comparing the coupling strengths between channels, as opposed to the proposed surrogate approach, may be biased due to channel specific features; for instance, channels located in the eloquent area might show higher values and the computed CFC might indicate normal function [19]. In our proposed method, the N_{CFC} was extracted by the PCA method across global PAC-grams. The N_{CFC} of whole seizure represents the repeatable and strong coupling pattern in seizure dynamics. Some studies suggested that tensor decomposition may be used for high dimensional decomposition [36]. Compared to such techniques, our measure provides a straightforward approach to reduce the high-dimensional PAC of all possible electrode pairs across frequency, effectively to determine the epileptogenic zone, as our assumption here is that ictal LFOs coupling with HFOs are the most dominant components in ictal epileptic networks. Additional tests showed that the precision went down while using second and third PCA components were included; from 92.5% of active HF hubs being located in the resected regions when using one component, to 79.2% and 68.3% when using 2 and 3 components, respectively (in the EC I group). The first component of PCA contains sufficient information for identifying pathological hubs with good performance (Fig. S6).

Other network measures mostly focus on exploring the causality of electrophysiological oscillations within specific frequency, so the higher and lower frequency activities are analyzed independently. Those measures ignore the interactions between high-frequency and low-frequency networks, which is an essential feature when modeling some pathological or physiological process [23], [37], [38]. The proposed N_{CFC} provides a chance for analyzing the interactions of higher and lower frequency epileptic networks in a unified framework to determine the role that HF or LF sub-networks play in ictal generation and propagation. This method can also be extended to other studies, such as memory network studies [39].

B. Pathological Hubs

Our results show that treatment, i.e. resection or ablation, of active HF hubs are correlated with improved outcome, which is in line with previous literature; suggesting HFO epileptic networks are critical in predicting surgical outcome [12]. However previous studies did not delineate whether HF hubs or LF hubs are more critical for predicting treatment outcomes. In our study, we modeled the HF and LF coupled CFC network, and the results show that HF hubs are superior to LF hubs in effectively locating epileptogenic tissues. 92.5% of active HF hubs resided in resected regions while this number decreased to 56.4% in LF hubs (Fig. 4(b), 4(d)) in patients with EC I outcome. Our analysis on the HFO networks and the LFO networks, independently, showed that only 58.8% of active HF hubs and 47.5% of active LF hubs resided in the resected regions of patients with EC I outcome (Fig. S4). Our study suggests that the active HF hubs of ictal N_{CFC} are pathological, which is also consistent with previous studies, and better captures the epileptogenic tissue than HFO or LFO networks that don't fully model cross-frequency coupling [11].

The HF hubs that emerged at early seizure stages tend to reside in the resected regions. As seizure starts propagating, other nodes outside the resected regions may also be recruited

into the epileptic network. The HF hubs of early stages correlate better with the resected regions in patients with favorable (EC I and II) outcome (Fig. 3(c)), compared to other stages. These results suggest that HFOs, early after seizure onset, may be limited to the seizure focus. As the strength of ictal discharges decrease, the focus gets weakened, and the widespread LF activity may modulate HF activity in other regions, such as the channels around PCC in patient P1 (Fig. 3(a)). The LF hubs of the late stage correlate better with the resected regions in the EC I group while the HF hubs of the late stage do not show significant differences between resected and non-resected regions (Fig. 3(c), 3(d)). This may explain previous findings that both HF and LF networks can be effective in identifying the pathological nodes [11], [17].

While previous studies have reported that CFC features from cortical sources of ECoG recordings can predict outcome [23], [25], our SEEG recording analysis showed that deep epileptogenic sources also demonstrate the CFC phenomenon. In the TLE and ETLE seizure-free patients, our results show that most identified active HF hubs were in deep structures. Most of the HF hubs in the TLE patients were located at the mesial temporal structure and the temporal pole region.

If one HF hub or LF hub always activated in separate seizures, the hub is more important for seizures propagation. There are seven patients with 3 seizures analyzed in EC I group. The times of repeated activation of HF hubs were counted during different stages, as shown in Fig. S7. The HF hubs in resected regions tended to be active repeatedly while the number of activated hubs decreases from one to three times in non-resected regions. To emphasize the importance of repeated pattern, we averaged the strengths of HF hubs or LF hubs if patients had more than one seizure.

C. HF Hubs for Targeting Treatment

Treating critical nodes of the epileptogenic network is correlated with favorable outcomes [11]. Nine patients achieved seizure-free outcome after surgical resections. The active HF hubs account for 23.7% of all resected nodes of these patients, which implies that the resection could be potentially reduced. However, the SEEG biomarker is only one of the important factors to localize epileptogenic zone. Other modalities, such as MRI, PET, seizure behavior, all contribute to the final surgical decision. One study demonstrated that limiting resections to brain areas with sustained ictal HFO activity achieves comparable success rates compared to standard larger resection treatments [40]. In our study, we speculate that these patients may also achieve good outcome while only resecting the critical hubs. Patient P6 achieved seizure-free outcome after RFTC. Two identified active HF hubs of this patient were all destroyed, which implies the importance of targeting treatment on the critical hubs. Apart from resection and RFTC, those hubs may also serve as target for neuromodulation therapies [41].

In our study, the SEEG recording was referenced to a selected intracranial contact on white matter with minimum activity. The focal onset may also spread to both hemispheres during seizure. The seizure activity may have strong influence on the reference electrode, as shown in Fig. S8(a). This 10 s SEEG segment was from the seizure of patient P1, as shown in Fig. 2(a). Those wide spread activities may be decreased by the bipolar montage, as shown in Fig. S8(c). We compared the N_{CFC} between the white matter reference and bipolar montage, as shown in Fig. S8(b) and S8(d), which represented the connectivity outside and inside the resected region, respectively. Only bipolar reference can correctly identify the resected areas. Therefore, we chose the more reliable bipolar montage at the price of decreasing spatial resolution.

D. Study Limitations

The N_{CFC} analysis supposed that epileptogenic network was under the coverage of SEEG implants, which may or may not be true; this may specifically determine the outcome in a patient. The choice for HF hubs in the N_{CFC} may be biased if SEEG recordings do not sufficiently cover the epileptogenic areas. The proposed method is for ictal data now, and it still needs more study on interictal data. The subdural is another widely used measure for recording brain electrical activity. Analyzing dataset with subdural recordings is our next research focus. It is also exciting to apply machine learning approach with validation on our dataset in the future. Prospective study is more powerful to test our proposed method in the real application, and it will be conducted to further advance the technology. Other limitations of the current work include the relatively small number of patients, and lack of larger multi-center datasets, which will be addressed in our future work.

ACKNOWLEDGMENT

The authors would like to thank Guanqian Yuan, Ping Huang, and Dandan Gao for providing clinical data support.

REFERENCES

[1] L. A. Baccalá, M. Y. Alvarenga, K. Sameshima, C. L. Jorge, and L. H. Castro, "Graph theoretical characterization and tracking of the effective neural connectivity during episodes of mesial temporal epileptic seizure," *J. Integrative Neurosci.*, vol. 3, no. 4, pp. 379–395, Dec. 2004.

[2] M. A. Kramer, E. D. Kolaczyk, and H. E. Kirsch, "Emergent network topology at seizure onset in humans," *Epilepsy Res.*, vol. 79, nos. 2–3, pp. 173–186, May 2008.

[3] F. Bartolomei *et al.*, "Defining epileptogenic networks: Contribution of SEEG and signal analysis," *Epilepsia*, vol. 58, no. 7, pp. 1131–1147, Jul. 2017.

[4] A. Sohrabpour, S. Ye, G. A. Worrell, W. Zhang, and B. He, "Noninvasive electromagnetic source imaging and Granger causality analysis: An electrophysiological connectome (eConnectome) approach," *IEEE Trans. Biomed. Eng.*, vol. 63, no. 12, pp. 2474–2487, Dec. 2016.

[5] A. Sohrabpour, Z. Cai, S. Ye, B. Brinkmann, G. Worrell, and B. He, "Noninvasive electromagnetic source imaging of spatiotemporally distributed epileptogenic brain sources," *Nature Commun.*, vol. 11, no. 1, Apr. 2020, Art. no. 1946.

[6] P. Xu *et al.*, "Differentiating between psychogenic nonepileptic seizures and epilepsy based on common spatial pattern of weighted EEG resting networks," *IEEE Trans. Biomed. Eng.*, vol. 61, no. 6, pp. 1747–1755, Jun. 2014.

[7] A. Bragin, J. Engel, and R. J. Staba, "High-frequency oscillations in epileptic brain," *Current Opinion Neurol.*, vol. 23, no. 2, pp. 151–156, Apr. 2010.

[8] J. Gotman, "High frequency oscillations: The new EEG frontier?" *Epilepsia*, vol. 51, no. 1, pp. 63–65, Feb. 2010.

[9] G. Worrell *et al.*, "Update on the mechanisms and roles of high-frequency oscillations in seizures and epileptic disorders," *Biomarkers Med.*, vol. 5, no. 5, pp. 557–566, Oct. 2011.

[10] P. Jiruska *et al.*, "High-frequency oscillations in epileptic brain," *Epilepsia*, vol. 58, no. 8, pp. 1330–1339, Aug. 2017.

[11] C. Wilke, G. Worrell, and B. He, "Graph analysis of epileptogenic networks in human partial epilepsy," *Epilepsia*, vol. 52, no. 1, pp. 84–93, Jan. 2011.

[12] S. Fuertinger, K. Simonyan, M. R. Sperling, A. D. Sharan, and F. Hamzei-Sichani, "High-frequency brain networks undergo modular breakdown during epileptic seizures," *Epilepsia*, vol. 57, no. 7, pp. 1097–1108, Jul. 2016.

[13] S. V. Gliske *et al.*, "Variability in the location of high frequency oscillations during prolonged intracranial EEG recordings," *Nature Commun.*, vol. 9, no. 1, Jun. 2018, Art. no. 2155.

[14] M. T. Kucewicz *et al.*, "High frequency oscillations are associated with cognitive processing in human recognition memory," *Brain*, vol. 137, no. 8, pp. 2231–2244, Aug. 2014.

[15] F. Brigo, "Intermittent rhythmic delta activity patterns," *Epilepsy Behav.*, vol. 20, no. 2, pp. 254–256, Feb. 2011.

[16] J. X. Tao *et al.*, "Interictal regional delta slowing is an EEG marker of epileptic network in temporal lobe epilepsy," *Epilepsia*, vol. 52, no. 3, pp. 467–476, Mar. 2011.

[17] S. B. Tomlinson, B. E. Porter, and E. D. Marsh, "Interictal network synchrony and local heterogeneity predict epilepsy surgery outcome among pediatric patients," *Epilepsia*, vol. 58, no. 3, pp. 402–411, Mar. 2017.

[18] N. von Ellenrieder, B. Frauscher, F. Dubeau, and J. Gotman, "Interaction with slow waves during sleep improves discrimination of physiologic and pathologic high-frequency oscillations (80–500 Hz)," *Epilepsia*, vol. 57, no. 6, pp. 869–878, Jun. 2016.

[19] Y. Nonoda *et al.*, "Interictal high-frequency oscillations generated by seizure onset and eloquent areas may be differentially coupled with different slow waves," *Clin. Neurophysiol.*, vol. 127, no. 6, pp. 2489–2499, Jun. 2016.

[20] Y. Iimura *et al.*, "Strong coupling between slow oscillations and wide fast ripples in children with epileptic spasms: Investigation of modulation index and occurrence rate," *Epilepsia*, vol. 59, no. 3, pp. 544–554, Mar. 2018.

[21] H. Motoi *et al.*, "Phase-amplitude coupling between interictal high-frequency activity and slow waves in epilepsy surgery," *Epilepsia*, vol. 59, no. 10, pp. 1954–1965, Oct. 2018.

[22] M. Amiri, B. Frauscher, and J. Gotman, "Interictal coupling of HFOs and slow oscillations predicts the seizure-onset pattern in mesiotemporal lobe epilepsy," *Epilepsia*, pp. 1160–1170, May 2019.

[23] S. A. Weiss *et al.*, "Seizure localization using ictal phase-locked high gamma: A retrospective surgical outcome study," *Neurology*, vol. 84, no. 23, pp. 2320–2328, Jun. 2015.

[24] G. M. Ibrahim *et al.*, "Dynamic modulation of epileptic high frequency oscillations by the phase of slower cortical rhythms," *Experim. Neurol.*, vol. 251, pp. 30–38, Jan. 2014.

[25] M. Guirgis, Y. Chinvarun, M. del Campo, P. L. Carlen, and B. L. Bardakjian, "Defining regions of interest using cross-frequency coupling in extratemporal lobe epilepsy patients," *J. Neural Eng.*, vol. 12, no. 2, Apr. 2015, Art. no. 026011.

[26] D. Jacobs, T. Hilton, M. del Campo, P. L. Carlen, and B. L. Bardakjian, "Classification of pre-clinical seizure states using scalp EEG cross-frequency coupling features," *IEEE Trans. Biomed. Eng.*, vol. 65, no. 11, pp. 2440–2449, Nov. 2018.

[27] C. Li *et al.*, "Epileptogenic source imaging using cross-frequency coupled signals from scalp EEG," *IEEE Trans. Biomed. Eng.*, vol. 63, no. 12, pp. 2607–2618, Dec. 2016.

[28] R. S. Fisher *et al.*, "Operational classification of seizure types by the international league against epilepsy: Position paper of the ILAE commission for classification and terminology," *Epilepsia*, vol. 58, no. 4, pp. 520–530, Apr. 2017.

[29] A. B. L. Tort, R. Komorowski, H. Eichenbaum, and N. Kopell, "Measuring phase-amplitude coupling between neuronal oscillations of different frequencies," *J. Neurophysiol.*, vol. 104, no. 2, pp. 1195–1210, Aug. 2010.

[30] D. Dvorak and A. A. Fenton, "Toward a proper estimation of phase–amplitude coupling in neural oscillations," *J. Neurosci. Methods*, vol. 225, pp. 42–56, Mar. 2014.

[31] J. Theiler, S. Eubank, A. Longtin, B. Galdrikian, and J. D. Farmer, "Testing for nonlinearity in time series: The method of surrogate data," *Phys. D, Nonlinear Phenomena*, vol. 58, nos. 1–4, pp. 77–94, Sep. 1992.

[32] O. Jensen, E. Spaak, and H. Park, "Discriminating valid from spurious indices of phase-amplitude coupling," *Eneuro*, vol. 3, no. 6, Nov. 2016, Art. no. e0334-16.

[33] F. Tadel *et al.*, "Brainstorm: A user-friendly application for MEG/EEG analysis," *Comput. Intell. Neurosci.*, Apr. 2011, Oct. 2011, Art. no. 879716.

[34] J. Aru *et al.*, "Untangling cross-frequency coupling in neuroscience," *Current Opinion Neurobiol.*, vol. 31, pp. 51–61, Apr. 2015.

[35] M. A. Kramer, A. B. L. Tort, and N. J. Kopell, "Sharp edge artifacts and spurious coupling in EEG frequency comodulation measures," *J. Neurosci. Methods*, vol. 170, no. 2, pp. 352–357, May 2008.

[36] E. Maris, M. van Vugt, and M. Kahana, "Spatially distributed patterns of oscillatory coupling between high-frequency amplitudes and low-frequency phases in human iEEG," *NeuroImage*, vol. 54, no. 2, pp. 836–850, Jan. 2011.

[37] H. Jiang, A. Bahramisharif, M. A. J. van Gerven, and O. Jensen, "Measuring directionality between neuronal oscillations of different frequencies," *NeuroImage*, vol. 118, pp. 359–367, Sep. 2015.

[38] H. Jiang, Z. Cai, G. A. Worrell, and B. He, "Multiple oscillatory push–pull antagonisms constrain seizure propagation," *Ann. Neurol.*, vol. 86, no. 5, pp. 683–694, Nov. 2019.

[39] N. Axmacher, M. M. Henseler, O. Jensen, I. Weinreich, C. E. Elger, and J. Fell, "Cross-frequency coupling supports multi-item working memory in the human hippocampus," *Proc. Nat. Acad. Sci. USA*, vol. 107, no. 7, pp. 3228–3233, Feb. 2010.

[40] P. N. Modur, S. Zhang, and T. W. Vitaz, "Ictal high-frequency oscillations in neocortical epilepsy: Implications for seizure localization and surgical resection," *Epilepsia*, vol. 52, no. 10, pp. 1792–1801, Oct. 2011.

[41] T. Yu *et al.*, "High-frequency stimulation of anterior nucleus of thalamus desynchronizes epileptic network in humans," *Brain*, vol. 141, pp. 2631–2643, Jul. 2018.